

# Identification of a Major Determinant for Serine-Threonine Kinase Phosphoacceptor Specificity

Catherine Chen,<sup>1,8</sup> Byung Hak Ha,<sup>1,8</sup> Anastasia F. Thévenin,<sup>1</sup> Hua Jane Lou,<sup>1</sup> Rong Zhang,<sup>1</sup> Kevin Y. Yip,<sup>2,3</sup> Jeffrey R. Peterson,<sup>4</sup> Mark Gerstein,<sup>2</sup> Philip M. Kim,<sup>5</sup> Panagis Filippakopoulos,<sup>6,7</sup> Stefan Knapp,<sup>6</sup> Titus J. Boggon,<sup>1</sup> and Benjamin E. Turk<sup>1,\*</sup>

<sup>1</sup>Department of Pharmacology, Yale University School of Medicine, New Haven, CT 06520, USA

<sup>2</sup>Department of Molecular Biophysics and Biochemistry, Yale University, New Haven, CT 06520, USA

<sup>3</sup>Department of Computer Science and Engineering, The Chinese University of Hong Kong, Shatin, New Territories, Hong Kong

<sup>4</sup>Division of Basic Science, Fox Chase Cancer Center, Philadelphia, PA 19111, USA

<sup>5</sup>Donnelly Centre for Cellular and Biomolecular Research, University of Toronto, Toronto, ON M5S 3E1, Canada

<sup>6</sup>Oxford University, Nuffield Department of Clinical Medicine, Target Discovery Institute (TDI) and Structural Genomics Consortium (SGC), Oxford OX3 7FZ, UK

<sup>7</sup>Ludwig Institute for Cancer Research, Old Road Campus Research Building, Oxford OX3 7DQ, UK

<sup>8</sup>These authors contributed equally to this work

\*Correspondence: [ben.turk@yale.edu](mailto:ben.turk@yale.edu)

<http://dx.doi.org/10.1016/j.molcel.2013.11.013>

This is an open-access article distributed under the terms of the Creative Commons Attribution License, which permits unrestricted use, distribution, and reproduction in any medium, provided the original author and source are credited.

Open access under [CC BY license](#).

## SUMMARY

Eukaryotic protein kinases are generally classified as being either tyrosine or serine-threonine specific. Though not evident from inspection of their primary sequences, many serine-threonine kinases display a significant preference for serine or threonine as the phosphoacceptor residue. Here we show that a residue located in the kinase activation segment, which we term the “DFG+1” residue, acts as a major determinant for serine-threonine phosphorylation site specificity. Mutation of this residue was sufficient to switch the phosphorylation site preference for multiple kinases, including the serine-specific kinase PAK4 and the threonine-specific kinase MST4. Kinetic analysis of peptide substrate phosphorylation and crystal structures of PAK4-peptide complexes suggested that phosphoacceptor residue preference is not mediated by stronger binding of the favored substrate. Rather, favored kinase-phosphoacceptor combinations likely promote a conformation optimal for catalysis. Understanding the rules governing kinase phosphoacceptor preference allows kinases to be classified as serine or threonine specific based on their sequence.

## INTRODUCTION

Proper signal transmission by protein kinases requires that they phosphorylate specific substrates at defined sites. Multiple mechanisms can act in concert to provide substrate specificity for kinases, including kinase-substrate colocalization, compart-

mentalization through the use of scaffold proteins, substrate recruitment through kinase adaptor subunits, and direct physical interactions between kinases and their substrates (Ubersax and Ferrell, 2007). In order for substrate phosphorylation to occur, the residue phosphorylated by the kinase must bind at least transiently to the catalytic cleft of the kinase. Accordingly, protein kinases tend to phosphorylate substrates in the context of consensus sequence motifs that have complementarity to the kinase active site (Pinna and Ruzzene, 1996). Such kinase phosphorylation site motifs play an important role in targeting kinases to specific substrates within the cell, as well as directing kinases to phosphorylate specific sites on their substrates.

One important aspect of the kinase phosphorylation site motif is the identity of the phosphorylation site residue itself. Almost all kinases in eukaryotes phosphorylate protein substrates on Ser, Thr, or Tyr residues. Ser-Thr kinases, which make up approximately 80% of the human kinome, comprise several groups phylogenetically distinct from Tyr-specific kinases (Manning et al., 2002). Accordingly, Ser-Thr kinases possess conserved signature residues within the catalytic domain important for accommodating a small, aliphatic phosphoacceptor residue at the active site (Taylor et al., 1995). Likewise, a distinct set of conserved residues characterizes Tyr kinases, which must accommodate a large, aromatic residue. Interestingly many, though not all, Ser-Thr kinases are significantly selective for either Ser or Thr as the phosphoacceptor residue (Pinna and Ruzzene, 1996). For example, cAMP-dependent protein kinase (PKA) strongly favors Ser over Thr in peptide substrates, and a large majority (>90%) of established *in vivo* phosphorylation sites are at Ser residues (Aimes et al., 2000; Kemp et al., 1977; Shabb, 2001). Conversely, the kinase LKB1 activates numerous downstream protein kinase substrates by phosphorylation exclusively on Thr residues (Lizcano et al., 2004). Although substrate specificity studies have predominantly been conducted *in vitro*, evidence is now emerging indicating that

phosphoacceptor residue identity significantly influences substrate phosphorylation efficiency in living cells (Kang et al., 2013). Thus, the presence of a preferred phosphoacceptor residue appears to be important for targeting of specific substrates by Ser-Thr kinases. However, the rules that govern this specificity are yet to be defined.

Here, we show that phosphoacceptor preference of Ser-Thr kinases is determined largely by the identity of a single residue, which we term “DFG+1.” This residue is located within the kinase activation segment, a conformationally flexible loop important for kinase regulation. Mutagenesis of this residue is sufficient to change the phosphoacceptor preference for kinases from distinct groups in a predictable manner. Identification of this residue therefore establishes a simple rule that can be used to predict phosphorylation site preference for a kinase of unknown specificity. We go on to show by X-ray crystallography of kinase-peptide complexes that conformation, rather than binding affinity, drives phosphoacceptor preference. Overall, these studies explain how a protein kinase is able to discriminate between Ser and Thr, two residues that differ only by a single methyl group.

## RESULTS

### A Residue within the Kinase Activation Loop Covaries with Phosphorylation Site Preference

We recently analyzed the peptide substrate specificity of a large number of Ser-Thr kinases from *S. cerevisiae* (Mok et al., 2010). Among these kinases, 32 preferred Ser, 10 preferred Thr, and 14 lacked substantial phosphoacceptor residue preference (Table S1 available online). While about half of the nonselective kinases belonged to a single phylogenetic group (the CDK-, MAPK-, GSK3-, and CKII-related [CMGC] kinase group), possibly attributable to a distinct peptide-binding mode (Brinkworth et al., 2003; Brown et al., 1999; Mok et al., 2010), all other kinase groups included both Ser- and Thr-specific kinases (Table S1 and Figure S1). Thus, in contrast to the clear distinction between Tyr kinases and Ser-Thr kinases, Ser-preferring and Thr-preferring kinases cannot be readily distinguished based on phylogeny.

Residues within the kinase catalytic domain that determine target specificity covary with corresponding residues in the substrate peptide (Li et al., 2003). Computational analysis of our yeast kinase data identified residues that covaried between kinases and their consensus peptide sequences (Yip et al., 2011). One residue correlating strongly with phosphoacceptor preference is found immediately downstream of a conserved Asp-Phe-Gly (DFG) sequence at the N terminus of the kinase activation loop (hereafter referred to as the DFG+1 residue). Consistent with a potential role in controlling kinase specificity, this residue is located within the substrate-binding cleft (Goldsmith et al., 2007). Among yeast kinases analyzed, Ser-selective kinases had larger hydrophobic residues (predominantly Leu, Phe, and Met) at this position, while most Thr-specific kinases had the  $\beta$ -branched aliphatic residue Ile at this position. All nonselective kinases had either Leu or Ser as the DFG+1 residue. This correlation was extended by inspection of additional human kinases (Table S2). For example, LKB1 and PDK1, which phosphorylate primarily Thr residues in substrates (Lizcano et al., 2004; Mora et al., 2004), have the  $\beta$ -branched residues

Val and Thr, respectively, at the DFG+1 position. In addition, human protein kinase C isozymes, which prefer Ser as the phosphoacceptor (Ferrari et al., 1985; House et al., 1987), have the straight-chain aliphatic residue Met at the analogous position. Based on its location within the kinase fold and the strong correlation between its identity and kinase specificity, we hypothesized that the DFG+1 residue might be an important determinant of phosphoacceptor specificity for Ser-Thr kinases.

### The DFG+1 Residue Controls Phosphoacceptor Specificity of Multiple Ser-Thr Kinase Families

Based on this hypothesis, mutation of the DFG+1 residue within Ser-Thr kinases should alter specificity in a predictable manner. We initially focused on human kinases in the Ste7-, Ste11-, and Ste20-related (STE) group. Most kinases in this group, including those in the mammalian Ste20-like (MST) kinase family, are Thr selective (Miller et al., 2008), while members of the p21-activated kinase (PAK) family are Ser selective (Rennefahrt et al., 2007). Phosphorylation site specificity within these families correlates with DFG+1 residue identity (Val for MST kinases and Phe for PAKs). We generated DFG+1 exchange mutants of these kinases (MST4<sup>V165F</sup> and PAK4<sup>F461V</sup>) and examined their phosphorylation specificity alongside their wild-type (WT) counterparts using optimized synthetic peptides that differ only at the phosphosite. As anticipated, WT MST4 preferentially phosphorylated the Thr peptide, while WT PAK4 preferentially phosphorylated the Ser peptide (Figure 1A and Table 1). Furthermore, mutation of the DFG+1 residue was sufficient to invert phosphorylation site specificity for both kinases on both consensus peptide substrates and peptide libraries (Figures 1A and S2). Notably, we found that for a given kinase, the  $K_m$  values for phosphorylation of the Ser and Thr peptides were similar, but phosphoacceptor residue identity had a large effect on  $k_{cat}$  (Table 1). These results suggest that phosphoacceptor preference is not mediated by differences in substrate binding affinity.

To determine whether the DFG+1 residue controls phosphoacceptor preferences among Ser-Thr kinases in general, we tested the effect of mutating this residue in two more distantly related kinases: Snf1 (the yeast ortholog of AMP-activated protein kinase, from the Ca<sup>2+</sup>/calmodulin-dependent protein kinase-related group) and PKA (from the PKA-, PKG-, and PKC-related [AGC] group). We generated a series of Snf1 mutants in which the DFG+1 residue (Leu198) was changed to residues most commonly found in other kinases at this position and evaluated the ability of these mutants to phosphorylate Ser- and Thr-containing peptides (Figure 1B). Mutation of Leu198 to a small or  $\beta$ -branched residue (Ser, Val, or Ile) converted it to a Thr kinase, while mutation to Phe in Snf1<sup>L198F</sup> retained a preference for Ser. Unexpectedly, Snf1<sup>L198M</sup>, predicted to be Ser specific, did not discriminate between Ser and Thr. For PKA, mutation of the DFG+1 residue (Phe187) to Val inverted its selectivity from Ser to Thr specific (Figure 1C). Taken together, these data indicate that the DFG+1 residue plays a predominant role in dictating phosphoacceptor specificity across multiple kinase groups.

If the DFG+1 residue is the primary determinant of Ser-Thr kinase phosphoacceptor specificity, the identity of this residue should allow us to predict the preference of an uncharacterized

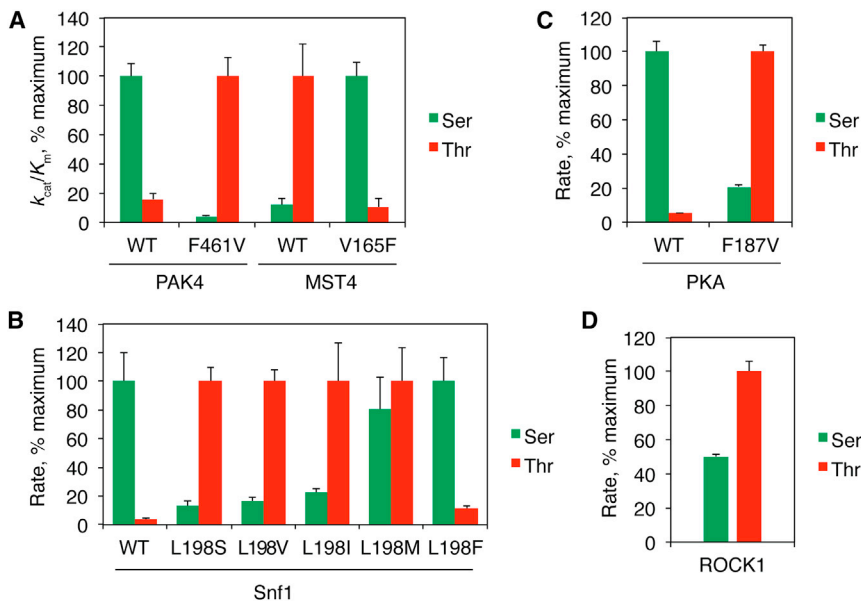


**Figure 1. The DFG+1 Residue Controls Ser-Thr Phosphosite Specificity**

For the kinases and peptide substrates indicated, the relative phosphorylation rates, as determined by radiolabel incorporation assay, are shown as a percentage of the maximally active substrate. The phosphorylation site residue is indicated by the color and location of the bar (Ser, green/left; Thr, red/right).

(A) PAK4 and MST4 DFG+1 mutants exchange phosphorylation site specificity. Relative  $k_{cat}/K_m$  values for WT PAK4, PAK4<sup>F461V</sup>, WT MST4, and MST4<sup>V165F</sup> were derived from data shown in Table 1.

(B) Relative reaction rates for phosphorylation of peptides with the sequence ALARAA(X) AAALAKKK at 40  $\mu$ M, where X is Ser or Thr as indicated, by yeast Snf1 and the indicated mutants. Results are the mean  $\pm$ SEM from three separate determinations.

(C) Relative rates of WT PKA and PKA<sup>F187V</sup> phosphorylation of 10  $\mu$ M peptide (GRRRRR(X) WYFGGK). Results show mean  $\pm$ SEM of triplicate samples from a representative experiment.

(D) Relative rates of phosphorylation of the peptides ARKRERAY(X)FGHHA at 5  $\mu$ M with the indicated phosphoacceptor residue by ROCK1. Results show mean  $\pm$ SEM of duplicate samples from a representative experiment. Absolute reaction rates for (B)–(D) are provided in Table S3. See also Figure S1 and Tables S1 and S2.

kinase. Most kinases within the human AGC group appear to prefer Ser, and in keeping with this, Leu, Met, and Phe are found most frequently at the DFG+1 position. Kinases in the ROCK family are outliers in that they have a  $\beta$ -branched Thr DFG+1 residue, suggesting they are likely to prefer Thr over Ser. Using a pair of matched peptides differing only at the phosphoacceptor site, we found that ROCK1 indeed had a significant (approximately 2-fold) preference for Thr as the phosphoacceptor (Figure 1D).

To assess the contribution of the DFG+1 residue to substrate phosphorylation in cells, we examined the ability of PAK4 to phosphorylate an established substrate, the proapoptotic protein BAD (Gnesutta et al., 2001), upon mutation of either PAK4 or its phosphorylation site in BAD (Ser112 to Thr, resulting in BAD<sup>S112T</sup>). Coexpression of WT PAK4 catalytic domain with BAD in HEK293 cells yields robust phosphorylation at Ser112 (Figure 2). Despite having similar catalytic parameters to the WT kinase in vitro on peptide substrates (see Table 1), PAK4<sup>F461V</sup> expression did not detectably induce WT BAD phosphorylation in cells above the background level. In contrast, PAK4<sup>F461V</sup> could phosphorylate BAD<sup>S112T</sup> in cells, but WT PAK4 phosphorylation of BAD<sup>S112T</sup> was substantially reduced. These results suggest that an optimal combination of phosphorylation site residue and DFG+1 residue is essential for maximal phosphorylation of at least some kinase substrates in living cells.

### The Structural Basis for Ser-Thr Kinase Phosphoacceptor Specificity

To understand the structural basis for how the DFG+1 residue controls phosphoacceptor specificity, we determined the X-ray cocrystal structures of WT and F461V mutant PAK4 catalytic domains in complex with consensus peptide substrates incorpo-

rating both their favored and disfavored phosphorylation site residues (PAKtide-S and PAKtide-T, Figure 3). We also determined an additional X-ray cocrystal structure of WT PAK4 with a longer version of the consensus peptide, PAKtide-S(L) (Figure S3). As previously observed for WT PAK4 in the absence of bound peptide (Eswaran et al., 2007; Ha et al., 2012), in each of the structures PAK4 is observed in the active state conformation with the activation loop phosphorylated on residue Ser474. The maximal root-mean-square deviation between the five structures is 1.1  $\text{\AA}$  over 290 C- $\alpha$  atoms (Table 2). Interestingly, the cocrystallized ATP analog was only visible in the electron density for the structure of the WT PAK4 complex with PAKtide-S (Figure S3). Both structures of WT PAK4 in complex with the optimal substrate, PAKtide-S or PAKtide-S(L), are highly similar, with small differences observed in the conformation of several side chains within the bound peptide and some crystal packing-induced conformational differences C-terminal to the phosphoacceptor residue (Figure S3). The bound peptide has a nearly identical backbone conformation, and, importantly, the residues most strongly selected by the kinase (the P-2 Arg and the P0 Ser residues [Rennefahrt et al., 2007; Zhu et al., 2005]) are observed in very similar orientations. As found in other structures of Ser-Thr kinases with bound peptide substrates (Brown et al., 1999; Bullock et al., 2005; Madhusudan et al., 1994; Yang et al., 2002), in both structures the Ser hydroxyl points toward the ATP binding site and is engaged in a network of polar contacts with conserved residues in the kinase catalytic loop (Figures 3A and S3L). Both structures therefore show the PAK4-peptide complex in a conformation apparently competent for phosphate transfer to occur. The DFG+1 Phe residue in these WT PAK4 structures is positioned within 4 $\text{\AA}$  of the Ser phosphoacceptor  $\beta$ -carbon and oriented perpendicular to the

**Table 1. Catalytic Constants for Phosphorylation of Peptide Substrates by PAK4 and MST4 and Their Exchange Mutants**

| Kinase                | Phosphoacceptor Residue | $k_{\text{cat}}$ ( $\text{s}^{-1}$ ) | $K_m$ ( $\mu\text{M}$ ) | $k_{\text{cat}}/K_m$ ( $\text{M}^{-1}\text{s}^{-1}$ ) |
|-----------------------|-------------------------|--------------------------------------|-------------------------|---|
| WT PAK4               | Ser                     | $0.097 \pm 0.015$                    | $280 \pm 20$            | $340 \pm 30$  |
|                       | Thr                     | $0.0089 \pm 0.0009$                  | $170 \pm 20$            | $54 \pm 12$   |
| PAK4 <sup>F461V</sup> | Ser                     | $0.0022 \pm 0.0001$                  | $129 \pm 3$             | $16.8 \pm 0.5$  |
|                       | Thr                     | $0.0301 \pm 0.0003$                  | $75 \pm 1$              | $400 \pm 50$  |
| WT MST4               | Ser                     | $0.6 \pm 0.2$                        | $21.7 \pm 0.7$          | $25,000 \pm 9,970$                                    |
|                       | Thr                     | $3.1 \pm 0.9$                        | $14 \pm 1$              | $210,000 \pm 46,000$                                  |
| MST4 <sup>V165F</sup> | Ser                     | $0.11 \pm 0.02$                      | $360 \pm 30$            | $310 \pm 30$  |
|                       | Thr                     | $0.013 \pm 0.002$                    | $390 \pm 90$            | $33 \pm 2$  |

Substrate peptides had the sequence GGRRRRRXWYFGGK for PAK4 and NKGYNXLRKK for MST4, where X was either Ser or Thr, as indicated above. Data show the mean of two separate experiments  $\pm$ SEM. See also Figure S2.

substrate peptide backbone (Figure 3B). This conformation for the DFG+1 Phe would preclude the additional methyl group of a Thr phosphoacceptor due to steric hindrance. Indeed, in the structure of WT PAK4 in complex with PAKtide-T, the bound peptide is in a nearly identical conformation. However, to accommodate the Thr phosphoacceptor residue, the DFG+1 Phe undergoes significant conformational movement: it rotates  $\sim 75^\circ$  about its  $\beta$ - $\gamma$  bond to allow the face of the Phe aromatic ring to interact with the Thr methyl group (Figure 3C). This conformation for the DFG+1 residue likely interferes with positioning of the  $\gamma$ -phosphate of ATP (Figures S3M–S3O). Consistent with the kinetic data, the structure does not suggest impaired PAKtide-T binding to the WT kinase. Rather, decreased phosphorylation of Thr substrates may occur due to conformational effects within the catalytic center. Taken together, these structures provide a likely explanation for why WT PAK4, and by extension other kinases with a DFG+1 Phe residue, is selective for Ser at the phosphorylation site.

To understand why kinases with a  $\beta$ -branched DFG+1 residue favor Thr, we examined the cocrystal structures of PAK4<sup>F461V</sup> in complex with PAKtide-S and with PAKtide-T. In the cocrystal structure of PAK4<sup>F461V</sup> with PAKtide-T, the phosphoacceptor Thr methyl group stacks snugly against the mutated DFG+1 Val residue, positioning the phosphoacceptor hydroxyl in an orientation similar to that observed in the WT PAK4-PAKtide-S complex (Figure 3D). The phosphoacceptor Thr appears poised for phosphate transfer, and thus the combination of Val at the DFG+1 position and Thr at the phosphoacceptor site seems to be highly accommodative to positioning an active-like conformation for the phosphoacceptor hydroxyl. In striking contrast, the cocrystal structure of PAK4<sup>F461V</sup> in complex with PAKtide-S displays an unexpected conformation of the phosphoacceptor Ser residue (Figure 3E). Although the overall peptide conformation is similar, the phosphoacceptor Ser is rotated about its  $\alpha$ - $\beta$  bond ( $\chi_1$ ) such that the hydroxyl group is pointed away from the active site. Additionally, two alternate conformations are observed for the DFG+1 Val residue. The PAK4<sup>F461V</sup> cocrystal structures therefore suggest that Val at the DFG+1 residue favors Thr over Ser because the additional methyl group allows interplay between the DFG+1 and phosphoacceptor residues, correctly positioning them to promote an optimal conformation for phosphate transfer.

## DISCUSSION

Our results suggest that discrimination by kinases between Ser and Thr involves control of proper conformation rather than binding to the active site. Our conclusion that Ser and Thr peptides bind with equal affinity is partly based on our observation that PAK4 and MST4 phosphorylate Ser and Thr substrates with similar  $K_m$  values. However, because the  $K_m$  value for an enzyme reaction is not necessarily equivalent to the substrate dissociation constant, substrate binding, conformation, and product release could all theoretically contribute to phosphoacceptor discrimination. We note, however, that Ser and Thr peptides appear to bind with equal affinity to the Ser-selective kinase PKA (Aimes et al., 2000). Discrimination between Tyr and Ser/Thr by kinases appears to involve differences in binding affinity as well as conformational control. X-ray crystal structures of Tyr kinases in complex with substrates have revealed favorable nonpolar interactions between the phosphoacceptor Tyr and conserved Tyr kinase-specific residues within the active site cleft (Favelyukis et al., 2001; Hubbard, 1997). In addition, Tyr kinases and Ser-Thr kinases differ in the conformation of the so-called P+1 loop, which interacts with the peptide backbone of a bound substrate to control its distance from the active site, thus dictating the size of the phosphoacceptor that can be accommodated (Hubbard, 1997; Taylor et al., 1995). Comparative kinetic analyses have been conducted for Ser and Tyr peptide phosphorylation by casein kinase 2 (CK2), a kinase that belongs to the CMGC Ser-Thr kinase group but that can also phosphorylate on Tyr residues, albeit with greatly reduced catalytic efficiency. These analyses revealed large (100-fold or more) differences in both  $k_{\text{cat}}$  and  $K_m$ , as well as distinct sequence preferences at residues flanking the phosphoacceptor (Marin et al., 1999; Vilk et al., 2008). These results suggest that Ser and Tyr peptides bind in distinct modes to the active site of CK2 and imply different binding affinities. In contrast, we found that Ser and Thr peptides bound to PAK4 with an identical backbone conformation and apparently comparable affinities.

The preference of a kinase for Ser or Thr, as reflected in peptide substrate phosphorylation *in vitro*, is likely to be generally important for substrate targeting *in vivo*. For example, we observed that most kinases in yeast prefer Ser, and based on the identity of their DFG+1 residues, most human kinases are

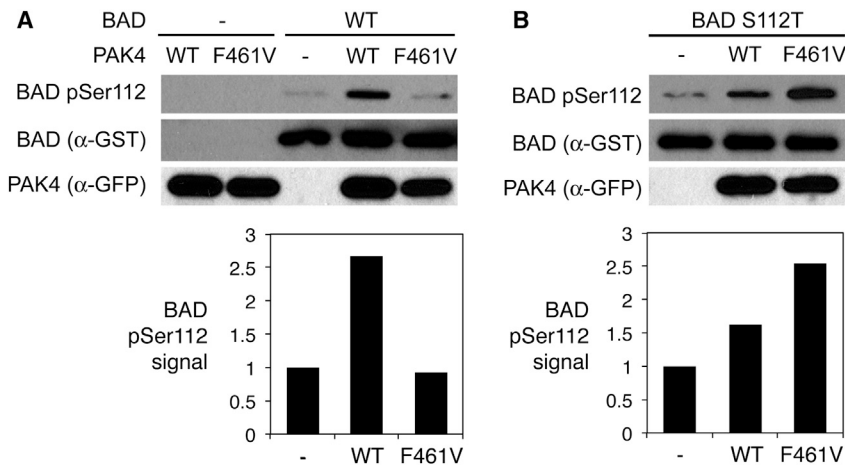


**Figure 2. The DFG+1 Residue Controls Protein Phosphorylation in Cells**

(A) GST-tagged BAD was transiently expressed in HEK293 cells with GFP-tagged WT PAK4 or PAK4<sup>F461V</sup> catalytic domain. Following serum starvation and treatment with wortmannin to reduce phosphorylation by endogenous kinases, GST-BAD was purified from cell lysates and analyzed by immunoblotting using phosphospecific antibodies. Quantified signal intensities for BAD pSer112 normalized to the total BAD signal are shown below as the ratio to the background signal.

(B) Phosphorylation of GST-tagged BAD<sup>S112T</sup> following coexpression with WT PAK4 and PAK4<sup>F461V</sup> was analyzed as in (A). A 5-fold greater quantity of BAD<sup>S112T</sup> compared to WT BAD was loaded on the gel to compensate for the reduced reactivity of the BAD pSer112 antibody.

predicted to prefer Ser as well. These observations suggest that the preponderance of pSer among yeast and human phosphoproteomes (Hornbeck et al., 2012; Sadowski et al., 2013) is related to intrinsic biochemical properties of eukaryotic kinases. For some kinases the presence of the preferred phosphoacceptor residue may constitute an essential component of its phosphorylation site motif. However, in many cases the preferred phosphoacceptor, while not absolutely required for phosphorylation by the kinase, may serve to confer robustness on substrate phosphorylation. For example, recent work has shown that exchanging Thr for Ser at sites of phosphorylation by the mTOR kinase could modulate sensitivity to activating stimuli or inhibitors of the kinase (Kang et al., 2013). In addition to influencing recognition by kinases, phosphorylation site identity can also influence downstream signaling as both protein phosphatases and phosphoprotein interaction domains can discriminate between pSer and pThr (Bremmer et al., 2012; Durocher et al., 2000).

While we have identified the DFG+1 residue as a major determinant for several kinases, other residues within the catalytic domain undoubtedly contribute to phosphoacceptor preference

as well. Individual kinases vary widely with respect to the stringency with which they discriminate between the two residues, and this is likely to be controlled by additional active site residues. For example, a residue in the glycine-rich loop located proximal to the  $\gamma$ -phosphate of bound ATP was shown to influence the extent to which PKA prefers Ser (Aimes et al., 2000). In addition, we found that a DFG+1 Leu residue correlated with Ser preference for most kinases, yet for kinases in the CMGC group it was associated with a lack of phosphoacceptor selectivity. Identification of additional “modifier” residues will facilitate a more complete understanding of structural features controlling kinase specificity. In addition, for some kinases it is possible that phosphorylation site specificity is entirely determined by other residues. Nonetheless, our current study suggests that, by inspection, one may determine whether a kinase is selective for Ser or Thr. To wit, a  $\beta$ -branched residue at the DFG+1 position appears to invariably dictate a preference for Thr, but Phe dictates preference for Ser as the phosphoacceptor residue. Our study therefore provides a much improved understanding of how protein kinases discriminate between phosphorylation site residues.

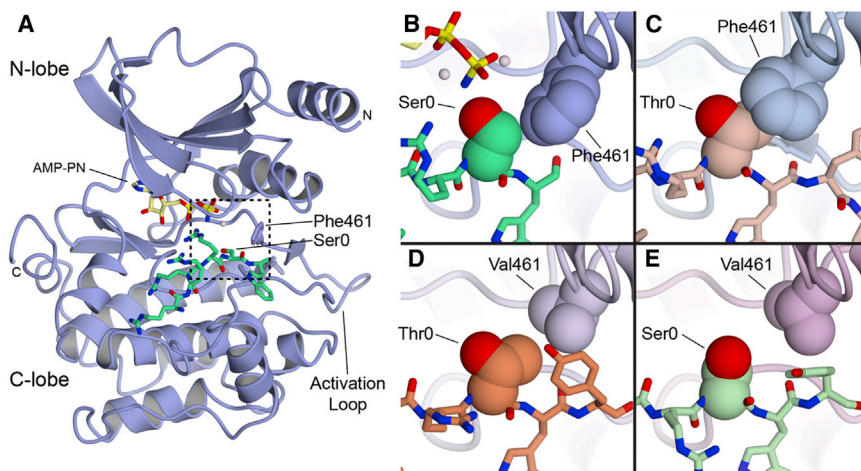


**Figure 3. Structural Analysis of PAK4 and PAK4<sup>F461V</sup> Complexes with PAKtide-S and PAKtide-T**

(A) Overall structure of PAK4 in complex with a PAKtide peptide. WT PAK4 with PAKtide-S is shown, with PAK4 in cartoon format and PAKtide-S in stick format. PAK4 is colored blue and PAKtide-S is colored green. DFG+1 residue Phe461 is indicated and shown in stick format. Phosphoacceptor residue Ser0 is indicated. Nucleotide is shown in stick format. Kinase N- and C-lobes are indicated. A box indicates the region shown in (B)–(E).

(B–E) Close-ups of (B) PAK4 WT with PAKtide-S, (C) PAK4 WT with PAKtide-T, (D) PAK4<sup>F461V</sup> with PAKtide-T, and (E) PAK4<sup>F461V</sup> with PAKtide-S are shown. The phosphoacceptor residue Ser0 or Thr0 and the DFG+1 residue Phe461 or Val461 are shown as spheres. Structural figures were generated using CCP4mg (McNicholas et al., 2011). See also Figure S3.

**Table 2. Data Collection and Refinement Statistics**

|   | PAK4 + PAKtide-T<br>PDB ID: 4JDH         | PAK4 + PAKtide-S<br>PDB ID: 4JDI         | PAK4 <sup>F461V</sup> + PAKtide-T<br>PDB ID: 4JDJ | PAK4 <sup>F461V</sup> + PAKtide-S<br>PDB ID: 4JDK | PAK4 + PAKtide-S(L)<br>PDB ID: 2Q0N      |
|---|--|--|---|---|--|
| Data Collection                                     |  |  |   |   |  |
| Space group   | <i>P</i> 4 <sub>1</sub> 2 <sub>1</sub> 2 | <i>P</i> 4 <sub>1</sub> 2 <sub>1</sub> 2 | <i>P</i> 4 <sub>1</sub> 2 <sub>1</sub> 2          | <i>P</i> 4 <sub>1</sub> 2 <sub>1</sub> 2          | <i>P</i> 4 <sub>3</sub> 2 <sub>1</sub> 2 |
| X-ray source and detector                           | NSLS X25 ADSC Q315                       | APS 24-ID-E ADSC Q315                    | NSLS X25 ADSC Q315                                | NSLS X25 ADSC Q315                                | SLS X10SA Mar-225                        |
| Wavelength (Å)                                      | 1.10000                                  | 0.97922                                  | 1.10000   | 1.10000   | 0.97910                                  |
| Unit cell: a, b, c (Å)                              | 61.9, 61.9, 179.4                        | 61.9, 61.9, 181.6                        | 61.8, 61.8, 181.7                                 | 61.6, 61.6, 180.8                                 | 145.7, 145.7, 39.6                       |
| α, β, γ (°)   | 90, 90, 90                               | 90, 90, 90                               | 90, 90, 90  | 90, 90, 90  | 90, 90, 90                               |
| Resolution range (Å) <sup>a</sup>                   | 50.0–2.0 (2.07–2.0)                      | 30.0–1.85 (1.92–1.85)                    | 50.0–2.3 (2.38–2.3)                               | 50.0–2.4 (2.49–2.4)                               | 50.0–1.75 (1.81–1.75)                    |
| Number of unique reflections                        | 24,692                                   | 31,180                                   | 30,247  | 14,691  | 40,410                                   |
| Completeness <sup>a</sup> (%)                       | 100 (100)                                | 99.9 (100)                               | 100 (99.8)  | 100 (100)   | 92.5 (94.2)                              |
| <i>R</i> <sub>sym</sub> (%) <sup>a</sup>            | 7.0 (119.0)                              | 9.1 (159.6)                              | 8.9 (69.0)  | 13.3 (96.4)                                       | 5.7 (35.5)                               |
| <i>R</i> <sub>pim</sub> (%) <sup>a</sup>            | 2.2 (34.9)                               | 3.0 (52.2)                               | 4.0 (36.7)  | 3.8 (25.0)  | –  |
| <i>R</i> <sub>rim</sub> (%) <sup>a</sup>            | 7.7 (124.1)                              | 9.2 (93.4)                               | 9.7 (79.4)  | 12.8 (81.7)                                       | –  |
| Mean σ <sup>a</sup>                                 | 27.9 (1.7)                               | 22.8 (1.8)                               | 17.5 (2.2)  | 17.4 (1.9)  | 16.3 (4.3)                               |
| Redundancy  | 12.4 (12.8)                              | 10.3 (10.5)                              | 6.0 (5.0)   | 11.9 (12.0)                                       | 12.0 (5.6)                               |
| Refinement Statistics                               |  |  |   |   |  |
| Resolution range (Å) <sup>a</sup>                   | 50.0–2.0 (2.05–2.0)                      | 30.0–1.85 (1.9–1.85)                     | 50.0–2.3 (2.36–2.3)                               | 50–2.4 (2.46–2.4)                                 | 32.6–1.75 (1.79–1.75)                    |
| <i>R</i> <sub>factor</sub> (%) <sup>a</sup>         | 18.3 (22.2)                              | 19.2 (26.6)                              | 19.5 (27.3)                                       | 18.5 (26.2)                                       | 18.2 (24.4)                              |
| Free <i>R</i> <sub>factor</sub> (%) <sup>a</sup>    | 22.4 (27.2)                              | 23.3 (27.2)                              | 24.4 (29.4)                                       | 24.9 (31.0)                                       | 22.8 (33.2)                              |
| Free <i>R</i> reflections (%) <sup>a</sup>          | 5.1 (5.6)                                | 5.1 (5.1)                                | 5.1 (8.0)   | 5.0 (6.8)   | 5.0 (5.7)                                |
| Free <i>R</i> reflections, number <sup>a</sup>      | 1,250 (70)                               | 1,568 (80)                               | 835 (67)  | 725 (49)  | 2,020 (159)                              |
| Residues built                                      |  |  |   |   |  |
| PAK4  | A/300–589                                | A/300–589                                | A/300–589   | A/300–589   | A/291–591                                |
| Cocrystallized peptide                              | B/–3 to 3                                | B/–4 to 1                                | B/–3 to 2   | B/–3 to 2   | B/–5 to 5                                |
| Number water molecules                              | 70                                       | 139                                      | 102   | 49  | 251                                      |
| Mean <i>B</i> factor (Å <sup>2</sup> )              |  |  |   |   |  |
| Protein (A)   | 45.5                                     | 35.5                                     | 39.3  | 48.0  | 24.0                                     |
| AMP-PN (A)  | –  | 30.9                                     | –   | –   | –  |
| Mg <sup>2+</sup> (A)                                | –  | 34.5                                     | –   | –   | –  |
| Peptide (B)   | 66.1                                     | 47.7                                     | 75.0  | 85.1  | 26.3                                     |
| H <sub>2</sub> O                                    | 47.0                                     | 40.3                                     | 39.2  | 46.5  | 34.1                                     |
| Model Statistics                                    |  |  |   |   |  |
| rmsd bond lengths (Å)                               | 0.019                                    | 0.008                                    | 0.007   | 0.014   | 0.016                                    |
| rmsd bond angles (°)                                | 2.007                                    | 1.328                                    | 1.179   | 1.803   | 1.588                                    |
| Ramachandran plot (%)<br>favored/allowed/disallowed | 98.3/1.7/0                               | 98.0/2.0/0                               | 97.9/2.1/0  | 97.2/2.8/0  | 98.1/1.9/0                               |

<sup>a</sup>High-resolution shell.

## EXPERIMENTAL PROCEDURES

### Protein Expression and Purification

PAK4, MST4, and PKA (WT and point mutants) were expressed with N-terminal hexahistidine tags in *E. coli* and purified by immobilized metal affinity chromatography. PAK4 and MST4 were further subjected to anion exchange, followed by size exclusion chromatography or size exclusion chromatography alone, respectively. GST-Snf1 (WT and mutant) was expressed in *E. coli*, purified by one-step glutathione affinity chromatography, and then activated by phosphorylation with recombinant Elm1 kinase, as described (Lee et al., 2012). Descriptions of expression vectors used and detailed purification procedures are provided in [Supplemental Experimental Procedures](#).

### Protein Kinase Assays

Kinase activity toward peptide substrates was determined by filter binding assay using radiolabeled ATP. Kinases were incubated with peptides and [ $\gamma$ -<sup>33</sup>P]ATP at 30°C for varying times, and aliquots were spotted on to P81 filter discs. Filters were quenched in 75 mM phosphoric acid and then washed three times for 4 min in 75 mM phosphoric acid, washed once briefly in acetone, air-dried, and analyzed by liquid scintillation counting. The amount of product formed was calculated from a standard curve made using [ $\gamma$ -<sup>33</sup>P]ATP at the same specific activity. Initial rates were determined by fitting the data to a line with Excel, and catalytic constants were calculated by fitting the initial velocity data to the Michaelis-Menten equation using KaleidaGraph software. Detailed procedures, including buffer compositions for each kinase reaction, are provided in [Supplemental Experimental Procedures](#).

**Cell Culture and Transfection**

HEK293 cells were cultured at 37°C and 5% CO<sub>2</sub> in Dulbecco's modified Eagle's medium containing 4.5 g/l D-glucose and L-glutamine (Invitrogen), 10% fetal bovine serum (FBS), and 1% penicillin/streptomycin. Cells in 6-well plates were cotransfected with 0.4 μg pEGFP-PAK4 catalytic domain and 3.6 μg pEBG-BAD using Lipofectamine 2000 (Invitrogen). After 24 hr, cells were exchanged into reduced serum medium (0.1% FBS) for 16 hr and treated with 250 nM wortmannin for 30 min prior to lysis. Cell lysates were prepared by washing briefly with PBS and extracting into lysis buffer (20 mM Tris-HCl [pH 7.5], 150 mM NaCl, 1 mM EDTA, 1 mM EGTA, 1% Triton X-100, 2.5 mM sodium pyrophosphate, 1 mM β-glycerophosphate, 1 mM Na<sub>3</sub>VO<sub>4</sub>, 1 mM DTT, 1 mM PMSF, 10 μg/ml leupeptin, 2 μg/ml pepstatin, and 10 μg/ml aprotinin) for 10 min at 4°C with rotation and centrifuging (10 min at 13,500 × g). GST-tagged BAD was purified from the supernatant with 20 μl glutathione Sepharose 4B suspension (GE Healthcare). Samples were subjected to SDS-PAGE followed by immunoblotting with α-BAD pSer112 antibody (Cell Signaling Technology #9291), α-GST antibody (Cell Signaling Technology #2624) and α-GFP antibody (Clontech #632381), and detection by enhanced chemiluminescence.

**Crystallography**

Crystals of WT PAK4 and PAK4<sup>F461V</sup> catalytic domain were obtained with both PAKtide-T (GGRRRRRTWYFGGGK) and PAKtide-S (RRRRRSWY) using the vapor diffusion hanging drop method. For WT PAK4 with peptides, we grew WT PAK4 crystals against 0.1 M Tris-HCl (pH 7.5) and 1.5–2.0 M NaOAc at room temperature and soaked with peptides. For PAK4<sup>F461V</sup> cocrystals with peptide, we grew against conditions of 0.1 M Tris-HCl (pH 7.5) and 1.5–2.0 M NaOAc at room temperature. For cocrystals of PAK4 in complex with PAKtide-S(L) (RRRRRSWYFDG), we grew against 1.7 M ammonium sulfate, 15% PEG400, and 0.1 M Tris-HCl (pH 8.0). Crystallographic data were collected at Advanced Photon Source (APS) beamline 24-ID-E, National Synchrotron Light Source (NSLS) beamline X25, or the Swiss light source beamline SLS-X10. Following structure solution, good electron density was observed for each of the kinase domains and their bound peptides.

**ACCESSION NUMBERS**

Crystallographic coordinates and structure factors are deposited in the PDB under accession codes 4JDH, 4JDI, 4JDJ, 4JDK, and 2Q0N.

**SUPPLEMENTAL INFORMATION**

Supplemental Information includes three figures, three tables, and Supplemental Experimental Procedures and can be found with this article online at <http://dx.doi.org/10.1016/j.molcel.2013.11.013>.

**ACKNOWLEDGMENTS**

We thank Reuben Shaw for helpful comments on the manuscript and Yang Deng for help with peptide synthesis. Beamline X25 at the National Synchrotron Light Source and Northeastern Collaborative Access Team at the Advance Photon Source are also thanked. This work was supported by NIH grants R01 GM102262 to T.J.B. and B.E.T., R01 GM105947 to B.E.T., R01 GM083025 to J.R.P., and Gilead Sciences grant YG-001-011 to T.J.B. Support for C.C. was provided by a training grant from the National Institutes of Health (T32 CA009085). S.K. is supported by the SGC, a registered charity (number 1097737) that receives funds from the Canadian Institutes for Health Research, the Canada Foundation for Innovation, Genome Canada, GlaxoSmithKline, Pfizer, Eli Lilly, Takeda, AbbVie, the Novartis Research Foundation, the Ontario Ministry of Research and Innovation, and the Wellcome Trust (092809/Z/10/Z). P.F. is supported by a Wellcome Trust Career-Development Fellowship (095751/Z/11/Z).

Received: September 11, 2013

Revised: October 24, 2013

Accepted: November 18, 2013

Published: December 26, 2013

**REFERENCES**

- Aimes, R.T., Hemmer, W., and Taylor, S.S. (2000). Serine-53 at the tip of the glycine-rich loop of cAMP-dependent protein kinase: role in catalysis, P-site specificity, and interaction with inhibitors. *Biochemistry* 39, 8325–8332.
- Bremmer, S.C., Hall, H., Martinez, J.S., Eissler, C.L., Hinrichsen, T.H., Rossie, S., Parker, L.L., Hall, M.C., and Charbonneau, H. (2012). Cdc14 phosphatases preferentially dephosphorylate a subset of cyclin-dependent kinase (Cdk) sites containing phosphoserine. *J. Biol. Chem.* 287, 1662–1669.
- Brinkworth, R.I., Breinl, R.A., and Kobe, B. (2003). Structural basis and prediction of substrate specificity in protein serine/threonine kinases. *Proc. Natl. Acad. Sci. USA* 100, 74–79.
- Brown, N.R., Noble, M.E., Endicott, J.A., and Johnson, L.N. (1999). The structural basis for specificity of substrate and recruitment peptides for cyclin-dependent kinases. *Nat. Cell Biol.* 1, 438–443.
- Bullock, A.N., Debreczeni, J., Amos, A.L., Knapp, S., and Turk, B.E. (2005). Structure and substrate specificity of the Pim-1 kinase. *J. Biol. Chem.* 280, 41675–41682.
- Durocher, D., Taylor, I.A., Sarbassova, D., Haire, L.F., Westcott, S.L., Jackson, S.P., Smerdon, S.J., and Yaffe, M.B. (2000). The molecular basis of FHA domain:phosphopeptide binding specificity and implications for phospho-dependent signaling mechanisms. *Mol. Cell* 6, 1169–1182.
- Eswaran, J., Lee, W.H., Debreczeni, J.E., Filipakopoulos, P., Turnbull, A., Fedorov, O., Deacon, S.W., Peterson, J.R., and Knapp, S. (2007). Crystal Structures of the p21-activated kinases PAK4, PAK5, and PAK6 reveal catalytic domain plasticity of active group II PAKs. *Structure* 15, 201–213.
- Favelyukis, S., Till, J.H., Hubbard, S.R., and Miller, W.T. (2001). Structure and autoregulation of the insulin-like growth factor 1 receptor kinase. *Nat. Struct. Biol.* 8, 1058–1063.
- Ferrari, S., Marchiori, F., Borin, G., and Pinna, L.A. (1985). Distinct structural requirements of Ca<sup>2+</sup>/phospholipid-dependent protein kinase (protein kinase C) and cAMP-dependent protein kinase as evidenced by synthetic peptide substrates. *FEBS Lett.* 184, 72–77.
- Gnesutta, N., Qu, J., and Minden, A. (2001). The serine/threonine kinase PAK4 prevents caspase activation and protects cells from apoptosis. *J. Biol. Chem.* 276, 14414–14419.
- Goldsmith, E.J., Akella, R., Min, X., Zhou, T., and Humphreys, J.M. (2007). Substrate and docking interactions in serine/threonine protein kinases. *Chem. Rev.* 107, 5065–5081.
- Ha, B.H., Davis, M.J., Chen, C., Lou, H.J., Gao, J., Zhang, R., Krauthammer, M., Halaban, R., Schlessinger, J., Turk, B.E., and Boggon, T.J. (2012). Type II p21-activated kinases (PAKs) are regulated by an autoinhibitory pseudosubstrate. *Proc. Natl. Acad. Sci. USA* 109, 16107–16112.
- Hornbeck, P.V., Kornhauser, J.M., Tkachev, S., Zhang, B., Skrzypek, E., Murray, B., Latham, V., and Sullivan, M. (2012). PhosphoSitePlus: a comprehensive resource for investigating the structure and function of experimentally determined post-translational modifications in man and mouse. *Nucleic Acids Res.* 40 (Database issue), D261–D270.
- House, C., Wettenhall, R.E., and Kemp, B.E. (1987). The influence of basic residues on the substrate specificity of protein kinase C. *J. Biol. Chem.* 262, 772–777.
- Hubbard, S.R. (1997). Crystal structure of the activated insulin receptor tyrosine kinase in complex with peptide substrate and ATP analog. *EMBO J.* 16, 5572–5581.
- Kang, S.A., Pacold, M.E., Cervantes, C.L., Lim, D., Lou, H.J., Ottina, K., Gray, N.S., Turk, B.E., Yaffe, M.B., and Sabatini, D.M. (2013). mTORC1 phosphorylation sites encode their sensitivity to starvation and rapamycin. *Science* 341, 1236566.
- Kemp, B.E., Graves, D.J., Benjamini, E., and Krebs, E.G. (1977). Role of multiple basic residues in determining the substrate specificity of cyclic AMP-dependent protein kinase. *J. Biol. Chem.* 252, 4888–4894.

- Lee, Y.J., Jeschke, G.R., Roelants, F.M., Thorner, J., and Turk, B.E. (2012). Reciprocal phosphorylation of yeast glycerol-3-phosphate dehydrogenases in adaptation to distinct types of stress. *Mol. Cell. Biol.* **32**, 4705–4717.
- Li, L., Shakhnovich, E.I., and Mirny, L.A. (2003). Amino acids determining enzyme-substrate specificity in prokaryotic and eukaryotic protein kinases. *Proc. Natl. Acad. Sci. USA* **100**, 4463–4468.
- Lizcano, J.M., Göransson, O., Toth, R., Deak, M., Morrice, N.A., Boudeau, J., Hawley, S.A., Udd, L., Mäkelä, T.P., Hardie, D.G., and Alessi, D.R. (2004). LKB1 is a master kinase that activates 13 kinases of the AMPK subfamily, including MARK/PAR-1. *EMBO J.* **23**, 833–843.
- Madhusudan, Trafny, E.A., Xuong, N.H., Adams, J.A., Ten Eyck, L.F., Taylor, S.S., and Sowadski, J.M. (1994). cAMP-dependent protein kinase: crystallographic insights into substrate recognition and phosphotransfer. *Protein Sci.* **3**, 176–187.
- Manning, G., Whyte, D.B., Martinez, R., Hunter, T., and Sudarsanam, S. (2002). The protein kinase complement of the human genome. *Science* **298**, 1912–1934.
- Marin, O., Meggio, F., Sarno, S., Cesaro, L., Pagano, M.A., and Pinna, L.A. (1999). Tyrosine versus serine/threonine phosphorylation by protein kinase casein kinase-2. A study with peptide substrates derived from immunophilin Fpr3. *J. Biol. Chem.* **274**, 29260–29265.
- McNicholas, S., Potterton, E., Wilson, K.S., and Noble, M.E. (2011). Presenting your structures: the CCP4mg molecular-graphics software. *Acta Crystallogr. D Biol. Crystallogr.* **67**, 386–394.
- Miller, M.L., Jensen, L.J., Diella, F., Jørgensen, C., Tinti, M., Li, L., Hsiung, M., Parker, S.A., Bordeaux, J., Sicheritz-Ponten, T., et al. (2008). Linear motif atlas for phosphorylation-dependent signaling. *Sci. Signal.* **1**, ra2.
- Mok, J., Kim, P.M., Lam, H.Y., Piccirillo, S., Zhou, X., Jeschke, G.R., Sheridan, D.L., Parker, S.A., Desai, V., Jwa, M., et al. (2010). Deciphering protein kinase specificity through large-scale analysis of yeast phosphorylation site motifs. *Sci. Signal.* **3**, ra12.
- Mora, A., Komander, D., van Aalten, D.M., and Alessi, D.R. (2004). PDK1, the master regulator of AGC kinase signal transduction. *Semin. Cell Dev. Biol.* **15**, 161–170.
- Pinna, L.A., and Ruzzene, M. (1996). How do protein kinases recognize their substrates? *Biochim. Biophys. Acta* **1314**, 191–225.
- Rennefahrt, U.E., Deacon, S.W., Parker, S.A., Devarajan, K., Beeser, A., Chernoff, J., Knapp, S., Turk, B.E., and Peterson, J.R. (2007). Specificity profiling of Pak kinases allows identification of novel phosphorylation sites. *J. Biol. Chem.* **282**, 15667–15678.
- Sadowski, I., Breitkreutz, B.J., Stark, C., Su, T.C., Dahabieh, M., Raithatha, S., Bernhard, W., Oughtred, R., Dolinski, K., Barreto, K., and Tyers, M. (2013). The PhosphoGRID *Saccharomyces cerevisiae* protein phosphorylation site database: version 2.0 update. Database (Oxford) **2013**, bat026.
- Shabb, J.B. (2001). Physiological substrates of cAMP-dependent protein kinase. *Chem. Rev.* **101**, 2381–2411.
- Taylor, S.S., Radzio-Andzelm, E., and Hunter, T. (1995). How do protein kinases discriminate between serine/threonine and tyrosine? Structural insights from the insulin receptor protein-tyrosine kinase. *FASEB J.* **9**, 1255–1266.
- Ubersax, J.A., and Ferrell, J.E., Jr. (2007). Mechanisms of specificity in protein phosphorylation. *Nat. Rev. Mol. Cell Biol.* **8**, 530–541.
- Vilk, G., Weber, J.E., Turowec, J.P., Duncan, J.S., Wu, C., Derksen, D.R., Zien, P., Sarno, S., Donella-Deana, A., Lajoie, G., et al. (2008). Protein kinase CK2 catalyzes tyrosine phosphorylation in mammalian cells. *Cell. Signal.* **20**, 1942–1951.
- Yang, J., Cron, P., Good, V.M., Thompson, V., Hemmings, B.A., and Barford, D. (2002). Crystal structure of an activated Akt/protein kinase B ternary complex with GSK3-peptide and AMP-PNP. *Nat. Struct. Biol.* **9**, 940–944.
- Yip, K.Y., Utz, L., Sitwell, S., Hu, X., Sidhu, S.S., Turk, B.E., Gerstein, M., and Kim, P.M. (2011). Identification of specificity determining residues in peptide recognition domains using an information theoretic approach applied to large-scale binding maps. *BMC Biol.* **9**, 53.
- Zhu, G., Fujii, K., Liu, Y., Codrea, V., Herrero, J., and Shaw, S. (2005). A single pair of acidic residues in the kinase major groove mediates strong substrate preference for P-2 or P-5 arginine in the AGC, CAMK, and STE kinase families. *J. Biol. Chem.* **280**, 36372–36379.